PNAS
www.pnas.org

Supplementary Information for

Phototaxis in a wild isolate of the cyanobacterium *Synechococcus elongatus*

Yiling Yang, Vinson Lam, Marie Adomako, Ryan Simkovsky, Annik Jakob, Nathan C. Rockwell, Susan E. Cohen, Arnaud Taton, Jingtong Wang, J. Clark Lagarias, Annegret Wilde, David R. Nobles, Jerry J. Brand, and Susan S. Golden

Susan S. Golden
Email: sgolden@ucsd.edu

This PDF file includes:

Supplementary text
Figs. S1 to S15
Tables S1 to S5
Captions for movies S1 to S8
References for SI reference citations

Other supplementary materials for this manuscript include the following:

Movies S1 to S8

www.pnas.org/cgi/doi/10.1073/pnas.1812871115

SI materials and methods

Plasmid and strain construction

All plasmids and strains are listed in Tables S3, S4 and S5. Transposon insertion mutants were constructed by homologous recombination following transformation of cyanobacterial strains with gene-specific cosmids from the *S. elongatus* PCC 7942 unigene set (UGS) library (1, 2). We designed plasmids for specific gene replacement as described elsewhere (3) using the CYANO_VECTOR server (http://golden.ucsd.edu /CyanoVECTOR/). Constructs for complementation of mutants were made by amplifying the target gene and inserting the fragment into the vector pAM5431 at a SwaI site; the resulting plasmid enables gene expression from genome Neutral Site I (NS1) under control of the P*trc* promoter. A YFP-tagged PixJ fusion was constructed by inserting *yfp* into pAM5477 with sequences that encode a GSGGG linker. All DNA fragments were assembled using an Invitrogen GeneArt seamless cloning kit (Thermo Fisher, Carlsbad, CA). Plasmid cloning was carried out in *Escherichia coli* strain DH5α using standard techniques.

Biofilm formation

S. elongatus strains grown on BG-11 agar plates were collected and used to inoculate 15-ml starter cultures grown in BG-11R (BG-11 with fresh iron and HEPES, as described in (4)) in 125-ml glass culture flasks. These starter cultures were grown shaking for 3 - 4 days at 30 °C under 150 µmol photons $m^{-2}s^{-1}$ illumination from fluorescent lights. Starter cultures were then diluted to OD 0.5 with BG-11R and 5 ml of this dilution was distributed to 25-ml glass culture flasks and placed in a stationary low-light (20 - 30 µmol photons $m^{-2}s^{-1}$) box at room temperature for 7 days to allow biofilm formation to occur. To assess biofilm formation, liquid cultures were slowly decanted, gently washed with water to remove unattached cells, stained with 5 ml of a 1% crystal violet solution for 15 min, washed again with water, and then allowed to dry.

Motility at different times of day

S. elongatus UTEX 3055 cells were cultured on BG-11 agar plates and entrained for two days in a 12-h light:12-h dark cycle before being released into constant light conditions at the end of the second dark period. Cells were harvested from the plate at 0.5, 12.5, 24.5, and 36.5 h after release into constant light and resuspended in fresh BG-11 medium. The cell suspension was flowed into a small chamber made from taped coverslips and cells were allowed to settle. Suspended cells were

removed by flowing in fresh BG-11 medium. Cell motility was observed on a Nikon TE300 inverted microscope at 40x magnification, with brightfield illumination provided by infrared LED at 850 nm wavelength. Cells were illuminated with oblique white-LED light. Images were acquired at 1-s intervals for 20 min. Cell tracking was performed using the Oufti software package (5). Cells that moved slower than 0.03 μm/s were regarded as non-motile and discarded from analysis.

Circadian bioluminescence monitoring

As described previously (6), *S. elongatus* strains expressing a P_{kaiBC}-*luc* reporter were grown at 30 °C for two cycles of 12-h light: 12-h dark to synchronize the population before transfer to constant-light conditions, during which bioluminescence was recorded every two hours. UTEX 3055 strains expressing the reporter gene from different neutral sites both showed bioluminescence rhythms similar to the corresponding PCC 7942 strains, with a period of 25 ± 0.4 h. Data were analyzed with the Biological Rhythms Analysis Software System (http://millar.bio.ed.ac.uk /PEBrown/BRASS/BrassPage.htm).

Immunoblot analysis

Equal amounts of total protein (5 μg) from each sample extract were separated by SDS-PAGE (AnykD, BIORAD), transferred to a polyvinylidene difluoride (PVDF) membrane, and blocked with 2.5% w/v nonfat dry milk / Tris Buffered Saline + 0.1 % Tween-20 (TBST). Membranes were incubated with α-GFP (mouse, Abgent) at 1:10,000 in 2.5% non-fat milk in TBST for 2 h, followed by five washes in TBST. Membranes were then incubated with horseradish peroxidase (HRP)-conjugated goat anti-mouse IgG secondary antibody (Thermo Scientific). Chemiluminescent detection was performed using Pierce SuperSignal West Femto detection reagents (Thermo Scientific).

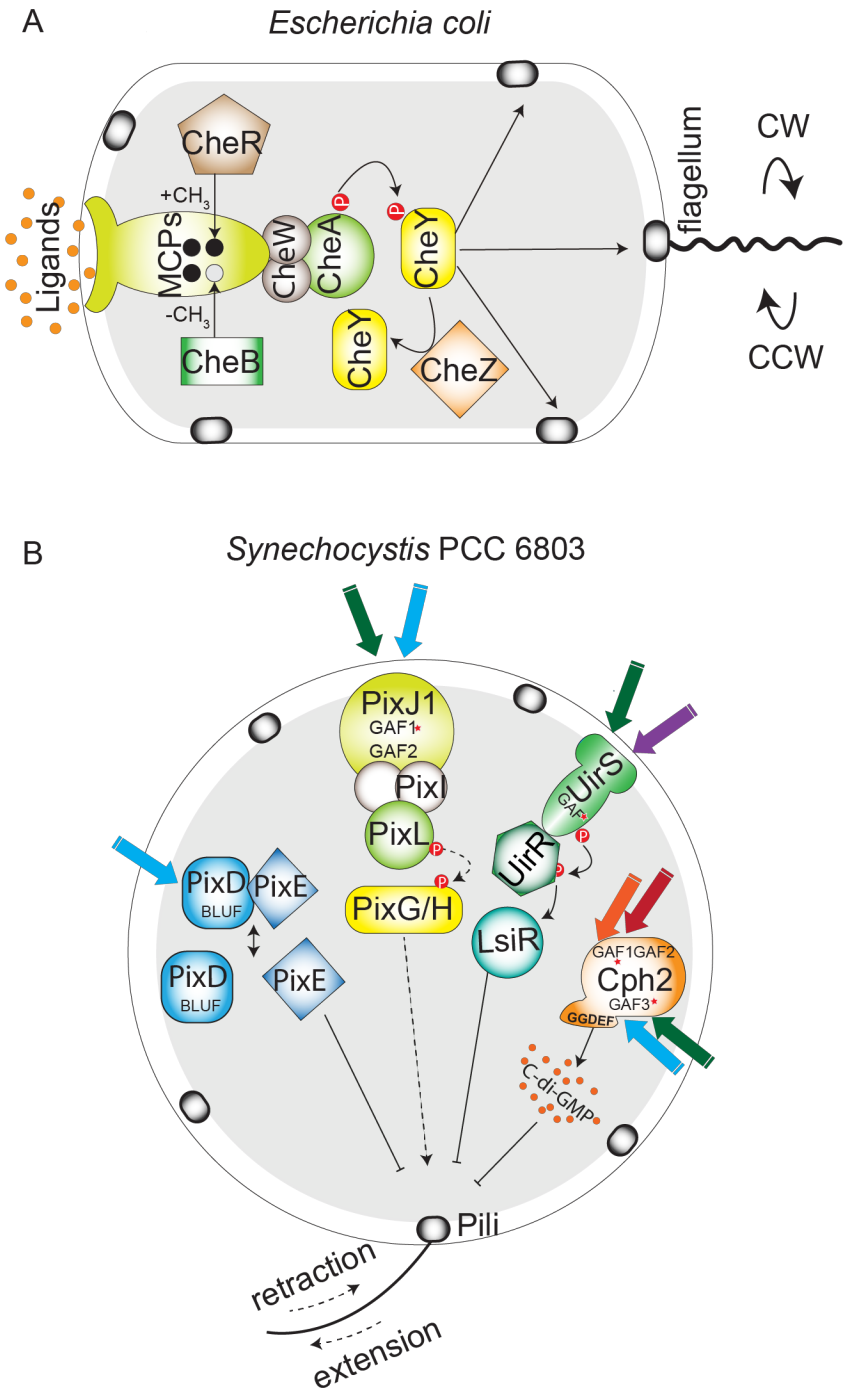

Fig. S1. Schematic illustration of chemotaxis signaling pathway in *E. coli* (A) and phototaxis pathways in *Synechocystis* PCC 6803 (B). *Synechocystis* employs homologs of *E. coli* chemotaxis proteins for sensing and regulation of phototaxis: MCP (PixJ1), CheA (PixL), CheW (PixI), and CheY (PixG/H). Adaptation proteins CheR and CheB, as well as phosphatase CheZ, are not encoded by cyanobacterial genomes. In addition to the Che-like pathway that senses blue and green light, *Synechocystis* contains other systems that control phototactic behavior. Notably, cyanobacteria move over solid surfaces through extension and retraction of type-IV pili that are distributed around the cell exterior (7, 8), whereas *E. coli* swim in liquid environments using flagella that rotate either clockwise (CW) or counterclockwise (CCW).

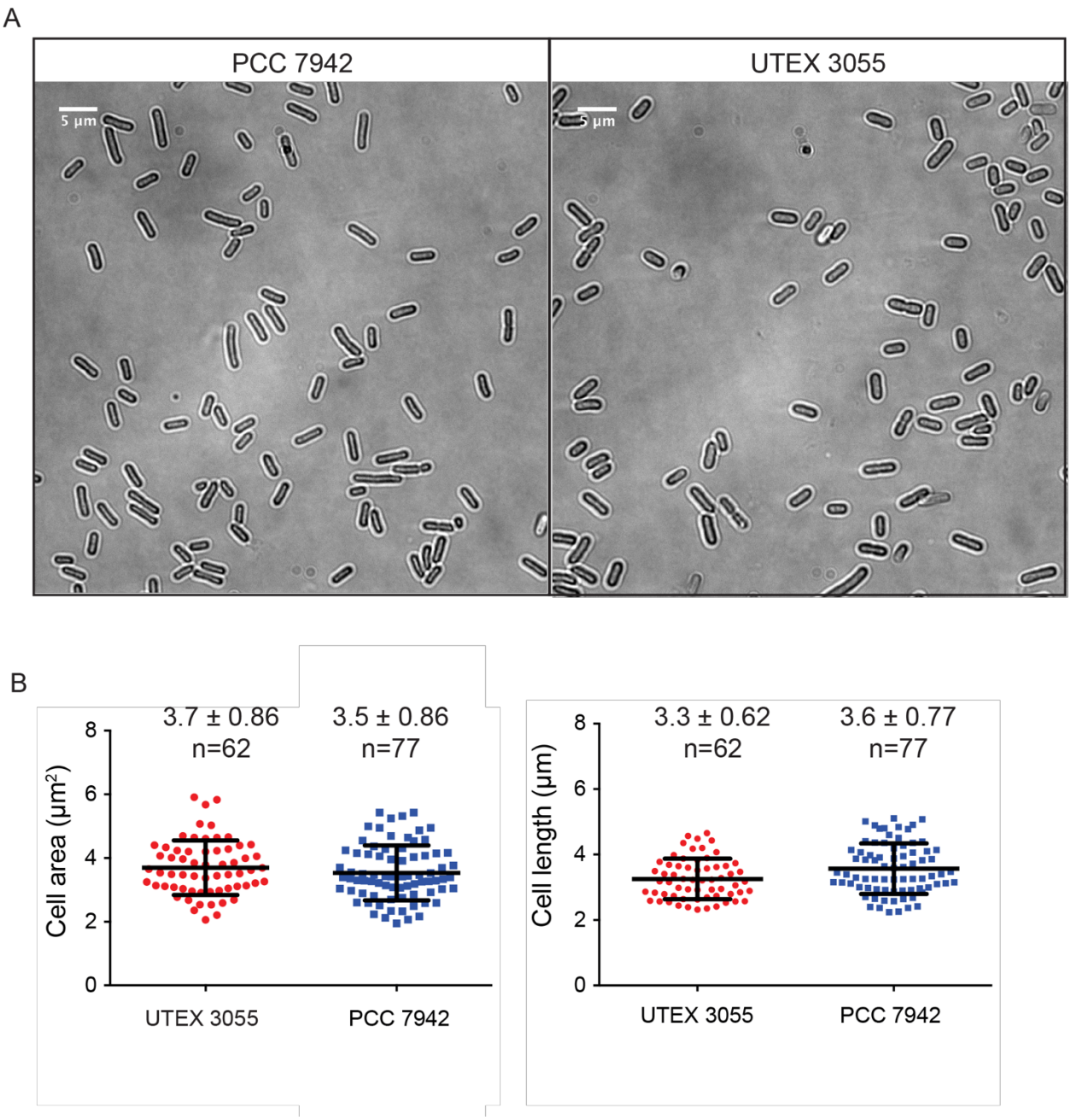

Fig. S2. Similar morphology of *S. elongatus* PCC 7942 and UTEX 3055. (A) Brightfield images of PCC 7942 and UTEX 3055. (B) Cell length and cell area of UTEX 3055 and PCC 7942 quantified from cells in (A). Bar represents mean with standard deviation (SD) and individual measurements are indicated by dots.

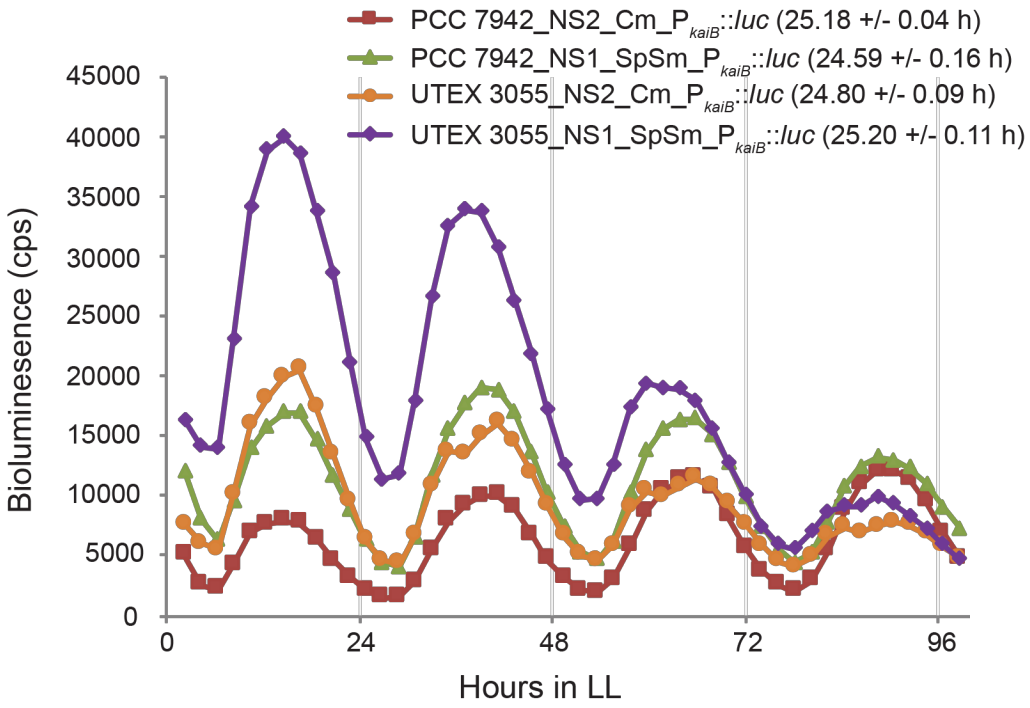

Fig. S3. Circadian rhythms of gene expression in *S. elongatus* PCC 7942 and UTEX 3055. Bioluminescence from strains carrying a P_{kaiB}-*luc* reporter at NS1 or NS2 was recorded as an assay for circadian rhythms of gene expression. The circadian period and standard error of the mean of each strain is indicated. LL, constant light after entrainment in a 12-h light:12-h dark cycle.

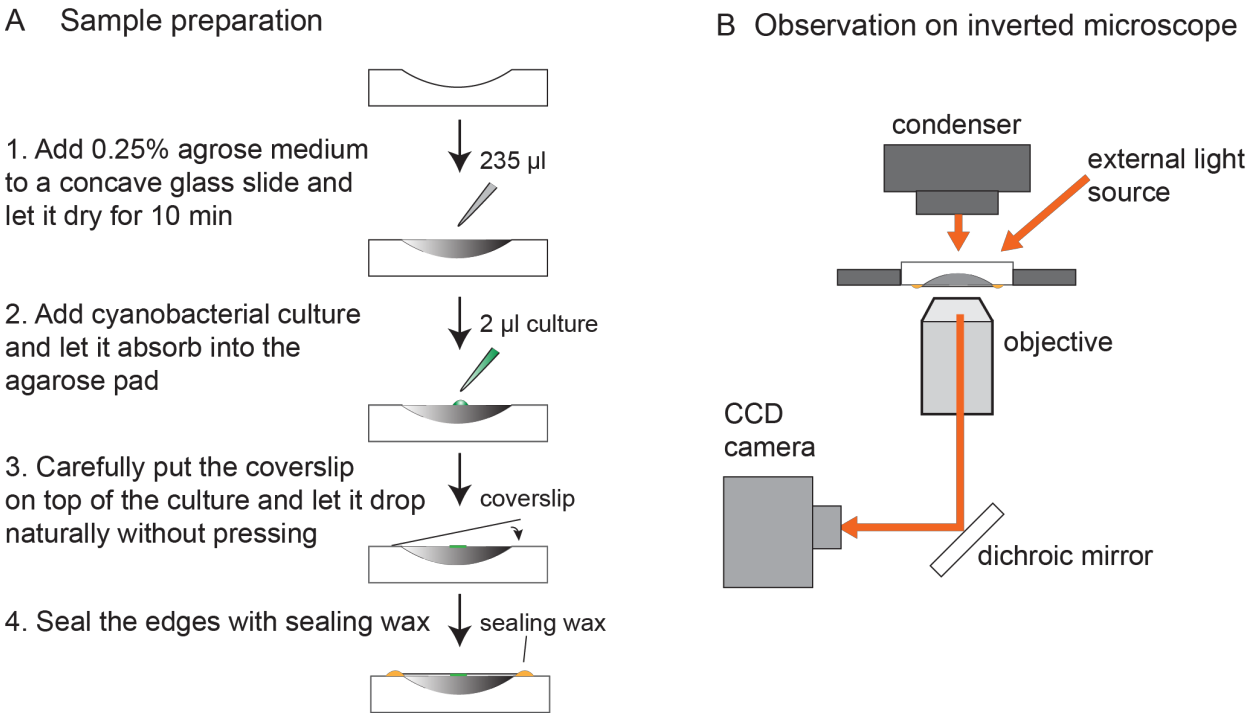

Fig. S4. Microscopic observation of cyanobacterial phototaxis. (A) Steps for cell sample preparation. (B) Observation of cell movement with inverted microscope under directional light provided by external light source or condenser light.

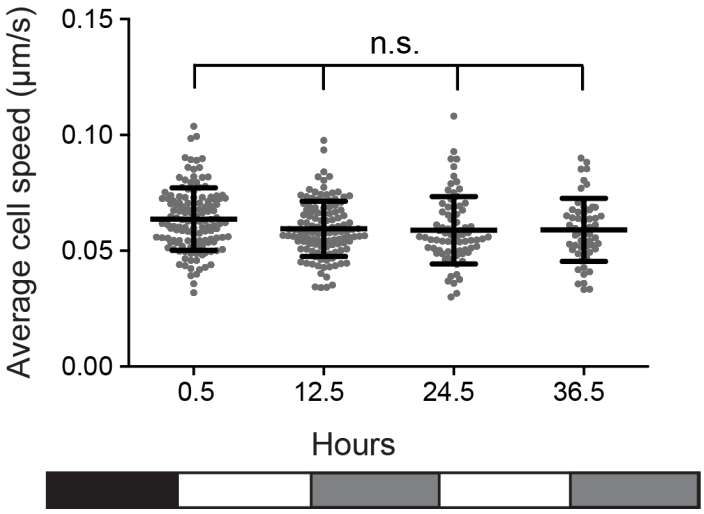

Fig. S5. Motility at different times of day. UTEX 3055 cell motility was monitored at the indicated time points in constant light following two days of entrainment in 12-h light:12-h dark cycles. The average cell speeds did not differ significantly at different time points. Dark box: dark night time; white box: subjective day; grey box: subjective night (circadian night in a light environment). 56-133 cells were measured at each time point; bar represents mean with SD. n.s.: not significant according to a one-way ANOVA test ($p > 0.05$).

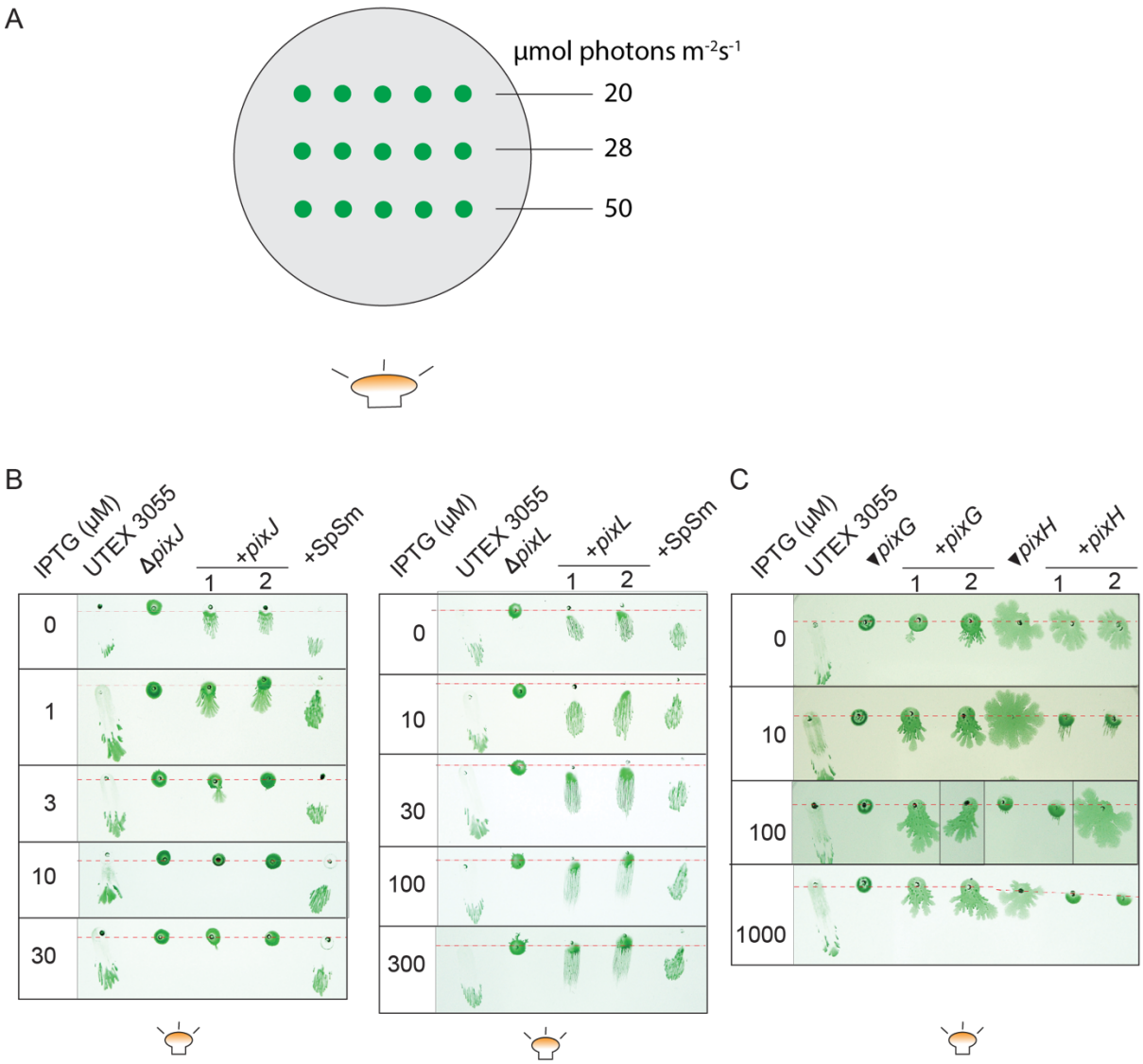

Fig. S6. Complementation of the phototaxis mutants. (A) Phototaxis assay setup. Green dots represent inoculation spots of *S. elongatus* cells, which were placed at different distances to the lateral light source. The fluence rate at each distance is noted. (B, C) Complementation of mutants *pixJ*, *pixL* (B) and *pixG*, *pixH* (C) by the respective genes under indicated level of IPTG induction. Two independent transformants were tested for each complementation assay. Empty vector expressing SpSm-resistance gene was introduced into UTEX 3055 at NS1 as a control. Red-dashed line indicates the starting position. Experiment was performed as in (A) and the representative results at 28 µmol photons $m^{-2}s^{-1}$ were presented.

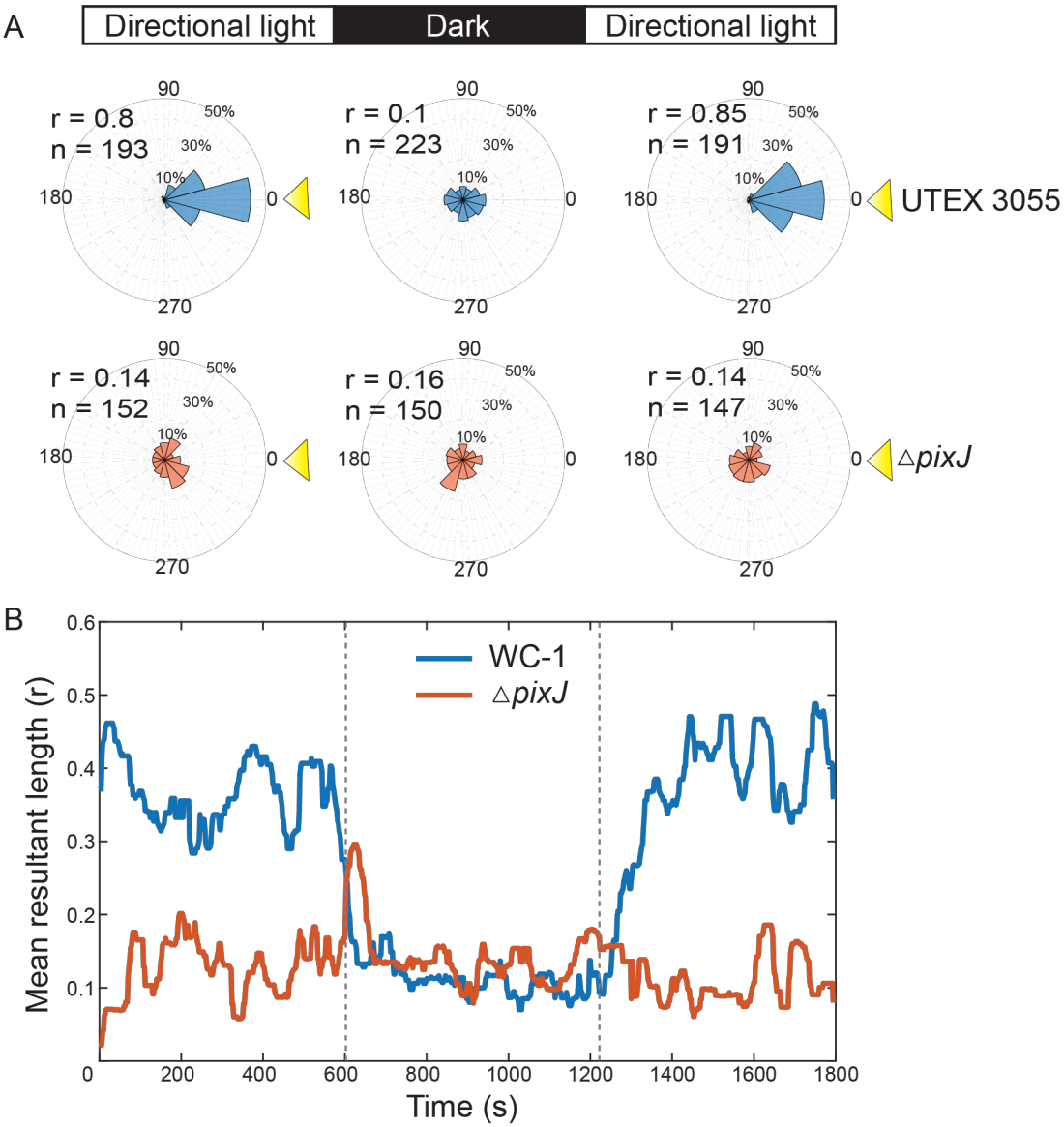

Fig. S7. Single-cell movement under lateral illumination and in the dark. Cell movement under directional illumination with a period of darkness for wild-type UTEX 3055 (blue) and Δ*pixJ* (orange). (A) Fraction of cells moving in a certain direction was quantified and plotted. (B) Mean resultant length 'r' from a Rayleigh test over time analyzed as in Fig. 1E. Dashed line indicates the time points of turning the lights off and on.

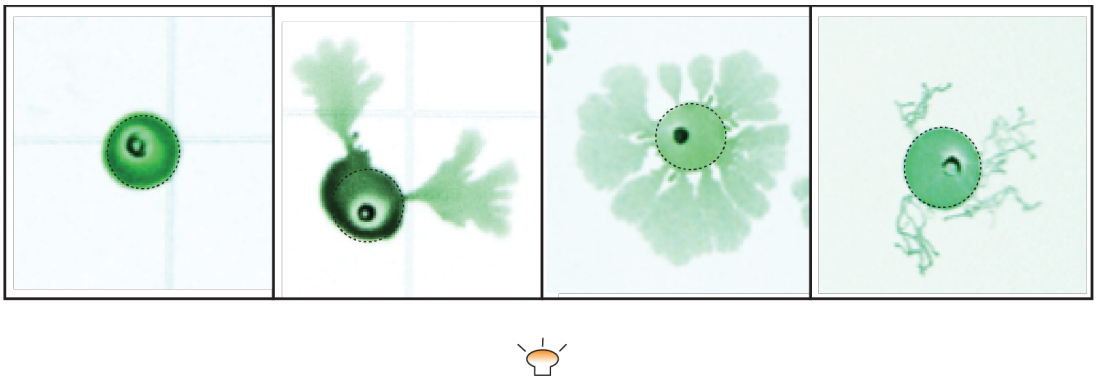

Fig. S8. Representative images of non-phototactic Δ*pixJ* cells on phototaxis plates. The appearance of the cell spots varied, even at different positions of the same assay plate. However, all samples showed loss of directional movement under a lateral light source. Light is coming in from the side indicated by a light bulb.

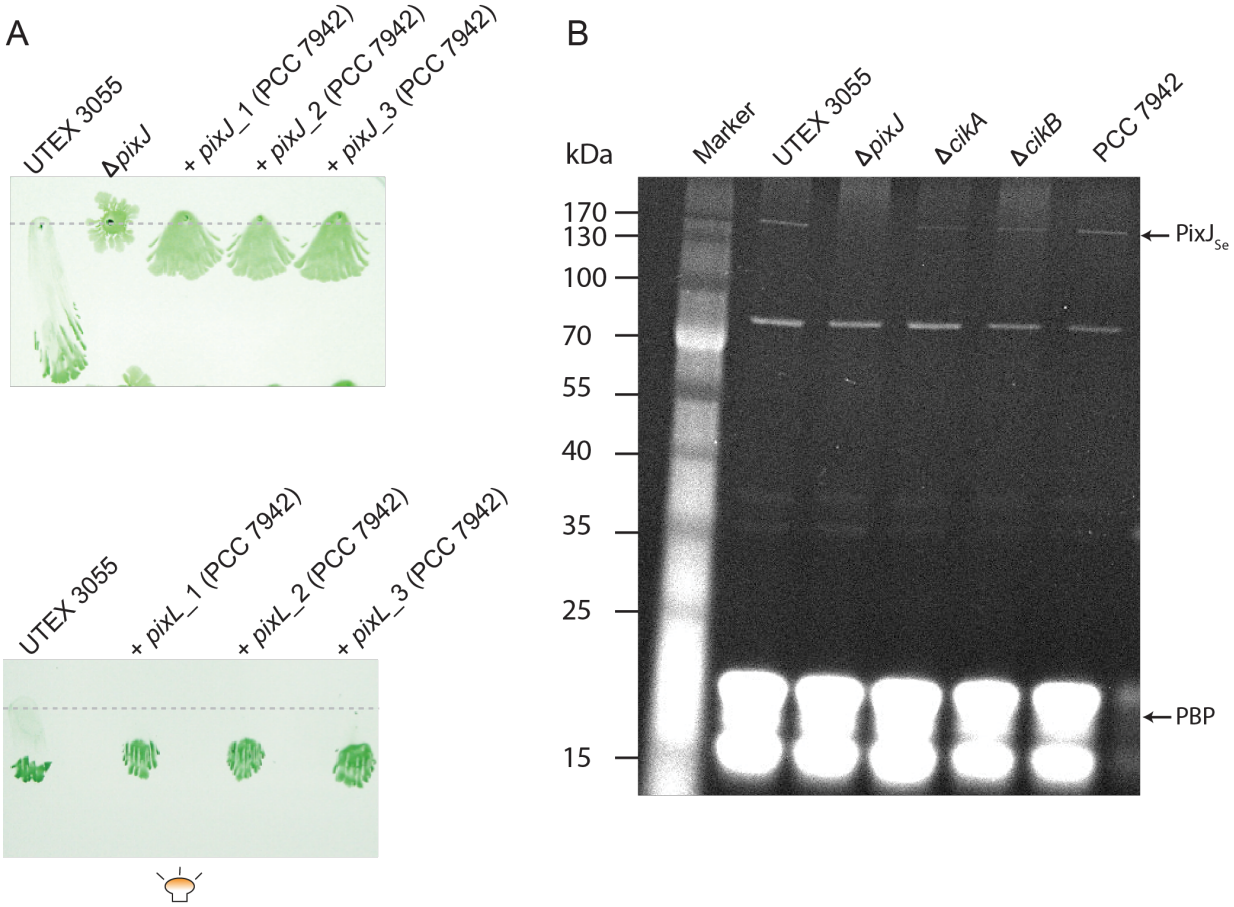

Fig. S9. Homologous proteins from PCC 7942 are functional in the respective UTEX 3055 mutants. (A) Expression of *pixJ* and *pixL* from PCC 7942 restored phototaxis to respective mutants of UTEX 3055. Three independent transformants marked as _1-3 were tested. A dashed line marks the point of inoculation. (B) Whole cell lysates of UTEX 3055, Δ*pix*J, Δ*cik*A, Δ*cik*B and PCC 7942 were separated by SDS-PAGE and tested for fluorescence in a zinc blot assay (9). The clock proteins *cikA* and *cikB* do not affect phototaxis but are included here to exclude the possibility that either is responsible for the 80 kDa zinc-reactive band. CikA and CikB are both approximately the same size as the PixJ band and each carries a GAF domain, but neither GAF is predicted to bind a bilin chromophore. Arrows indicate positions of $PixJ_{Se}$ and phycobiliproteins (PBP). This result showed that PCC 7942 expresses a bilin-binding PixJ homolog at a similar level as that of UTEX 3055.

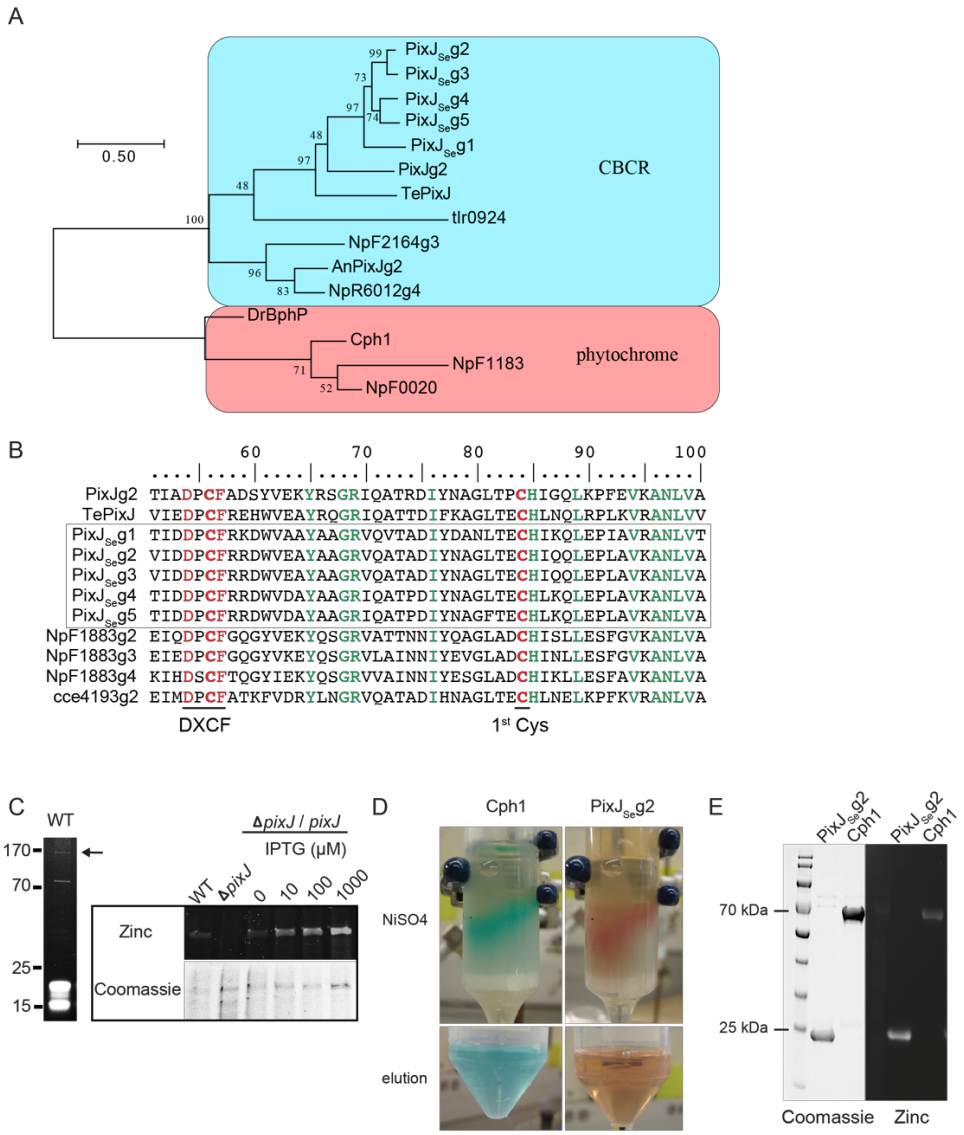

Fig. S10. Classification of PixJ$_{Se}$ and purification of the second GAF domain. (A) Phylogenetic tree of GAF domains from PixJ$_{Se}$ and bilin-binding photoreceptors from other species: *Synechocystis* (Cph1and PixJg2); *Thermosynechococcus elongatus* BP-1 (Te); *Anabaena sp.* PCC 7120 (An); *Nostoc punctiforme* ATCC 29133 (NpF/NpR); *Deinococcus radiodurans* (Dr). Phylogenetic analysis was performed using the maximum-likelihood method. Cyanobacteriochromes are shaded in blue and phytochromes are shaded in pink. Number of bootstrap replications is 500. Bootstrap values are shown. (B) All GAF domains in PixJ$_{Se}$ show high similarity to DXCF CBCR. GAF domain sequences of PixJ$_{Se}$ (g1-g5) were aligned to known DXCF CBCRs. Conserved Cys residues and "DXCF" module are highlighted in red and identical sequences are shown in green. *Cyanothece* sp. ATCC 5114 (cce4193g2). (C) Presence of bilin-bound protein detected by zinc-blot assay in UTEX 3055, Δ*pixJ* and complemented strain under indicated level of IPTG induction. (D) Nickel-affinity chromatography. Cell lysates containing Cph1(N514)-His or PixJ$_{Se}$GAF2-His in presence of phycocyanobilin (PCB) exhibits cyan or pink color, respectively, when passing through the nickel column. (E) SDS gel and zinc blot of purified Cph1(N514)-His and PixJ$_{Se}$GAF2-His protein obtained from (D).

A

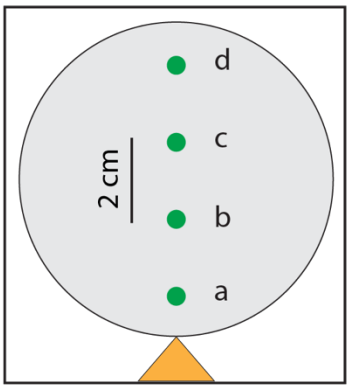

	LED (μm photons m^{-2} s^{-1})							
	W	B	G	R	RB	RG	BG	RGB
d	13	2.5	2.5	2.5	5	5	5	7
c	17	4	4	5	7	7	7	12
b	24	6	6	7	12	11	12	20
a	40	20	20	21	35	35	34	50

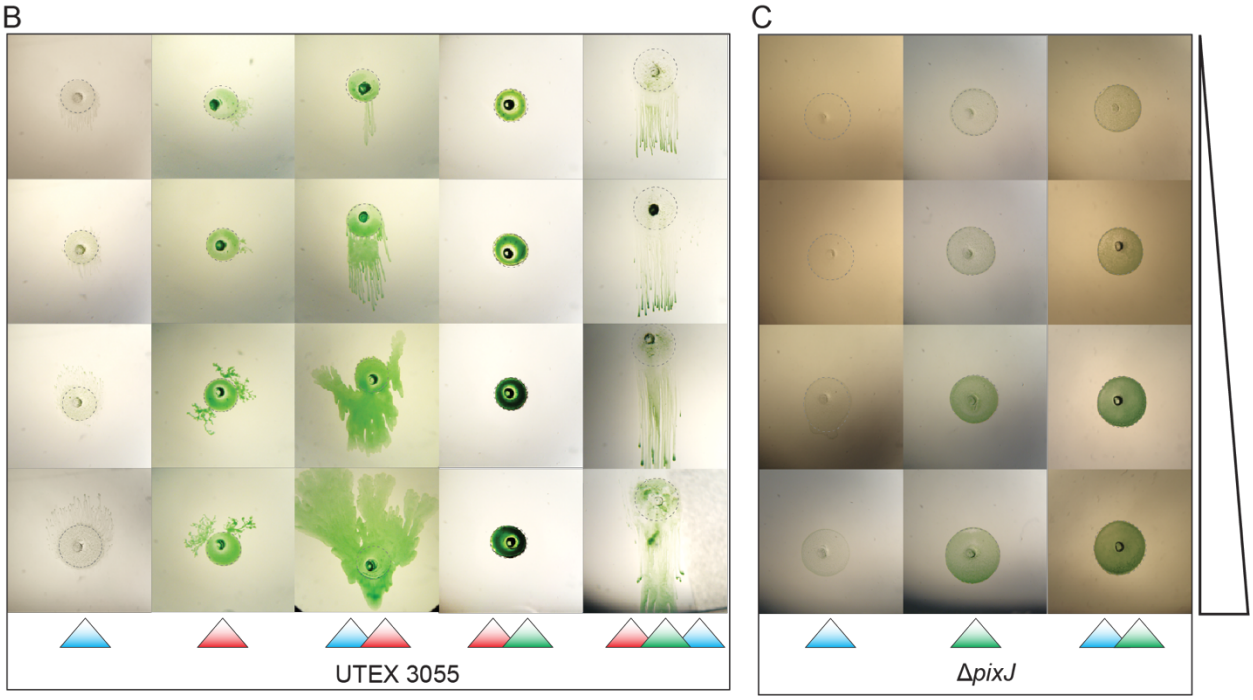

Fig. S11. Phototactic response of UTEX 3055 to different colors of light. (A) Schematic drawing of the experimental design. Grey area represents a Petri dish filled with soft BG-11 medium and the green dots represent inoculation spots of *S. elongatus* cells. The Petri dish was placed in a black box with an LED bulb (clear white or 5-mm RGB controllable from microtivity) mounted on one sidewall indicated by an orange triangle. Cells were placed at different distances (a, b, c and d) from the light bulb and the total irradiance level at each position measured with a photometer (Biospherical Instrument QSL-100) is listed on the right for each lighting condition. W, white; R, red; G, red; B, blue. red, λ=630 nm, FWHM (full width at half maximum) =25 nm; blue, λ=465 nm, FWHM =25 nm; green λ=516 nm, FWHM=30 nm. (B) Phototactic migration of wild-type UTEX 3055 toward single color or additive colors of LED light as indicated. (C) Cells of a *pixJ* mutant do not show phototaxis to either individual or a combination of blue and green light. All

experiments were performed for at least three replicates and representative results are shown. Triangle at right indicates fluence gradient. Tree-like twisted branches formed under red light in panel A indicate non-directional movement as shown in Fig. S8.

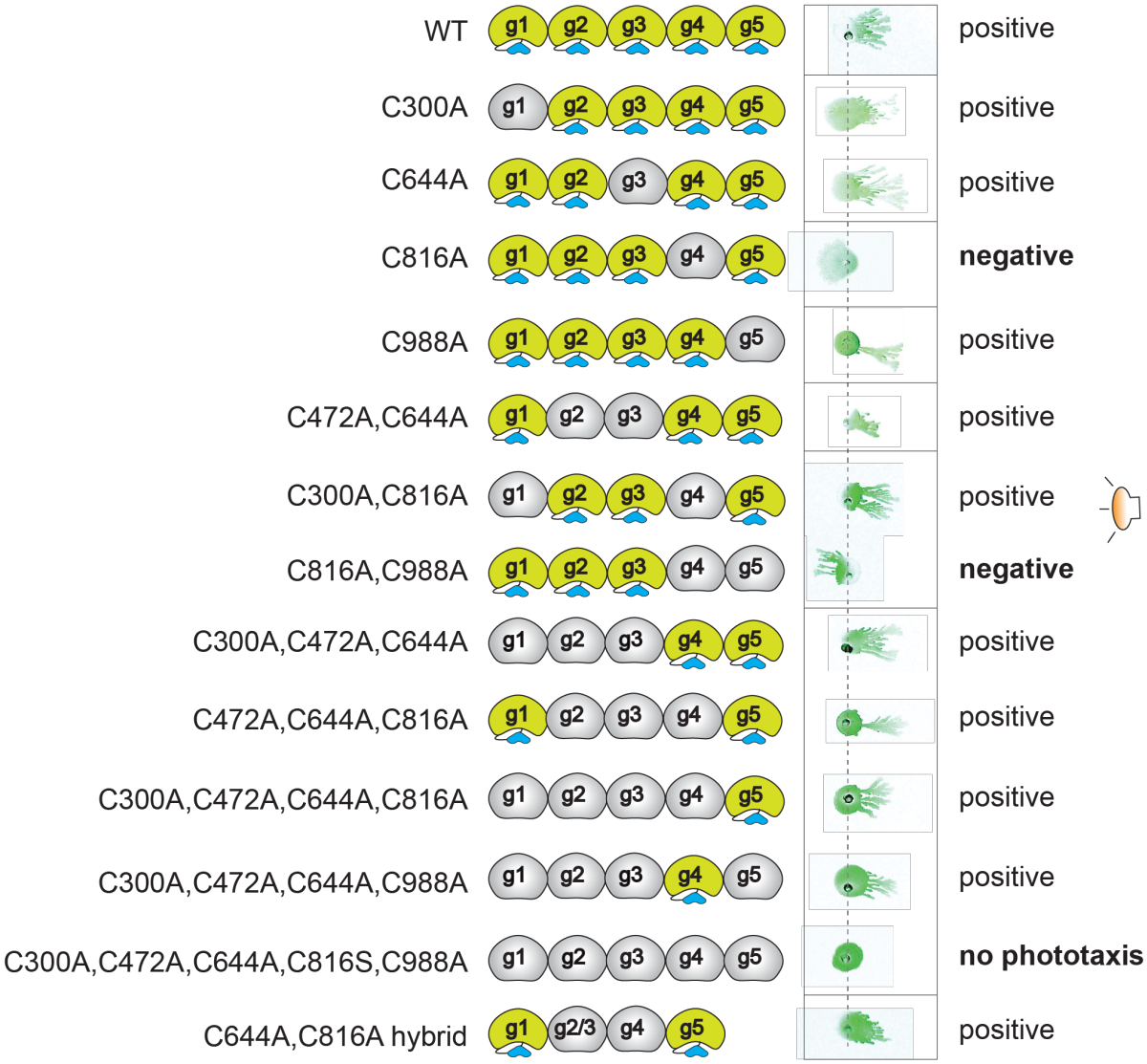

Fig. S12. Phototaxis phenotypes of all $PixJ_{Se}$ variants that carry Cys➔Ala mutations in specific GAF domains. Intact GAFs are shown in yellow and GAF domains with the first conserved Cys mutated to Ala are shown in gray. Representative image of phototaxis phenotype of each mutant is shown on the right. Images of cells taken from different plates are separated by solid black lines. Dashed line indicates the inoculation position of cells with directional white light provided from the right (See Fig. S6A for experimental setup). All assays were performed at least three times with the indicated outcomes.

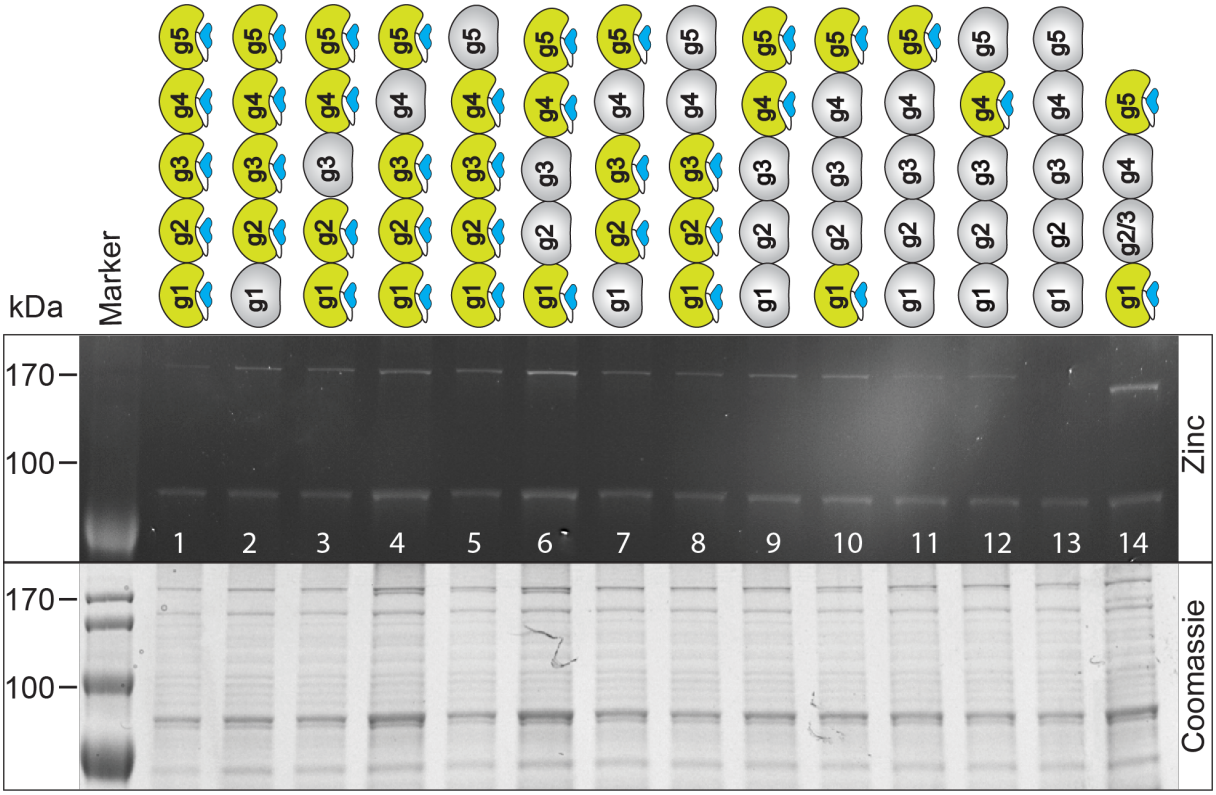

Fig. S13. Bilin-binding ability of $PixJ_{Se}$ variants with substitution of Cys ➔Ala in different GAF domains. Lane 1: Wild-type UTEX 3055; lanes 2-14: UTEX 3055 *pixJ* mutant expressing $PixJ_{Se}$ variants represented by schematic GAF domains with or without bilin. Note that the mutant in lane 14 expresses $PixJ_{Se}$ with a lower molecular weight due to presence of only four GAF domains, in which the first half of GAF2 and the second half of GAF3 were fused together through a cloning artifact. Zinc stain of SDS-PAGE gel of proteins from lysates of indicated strains (upper panel). Coomassie staining of proteins in the same SDS-PAGE gel (lower panel).

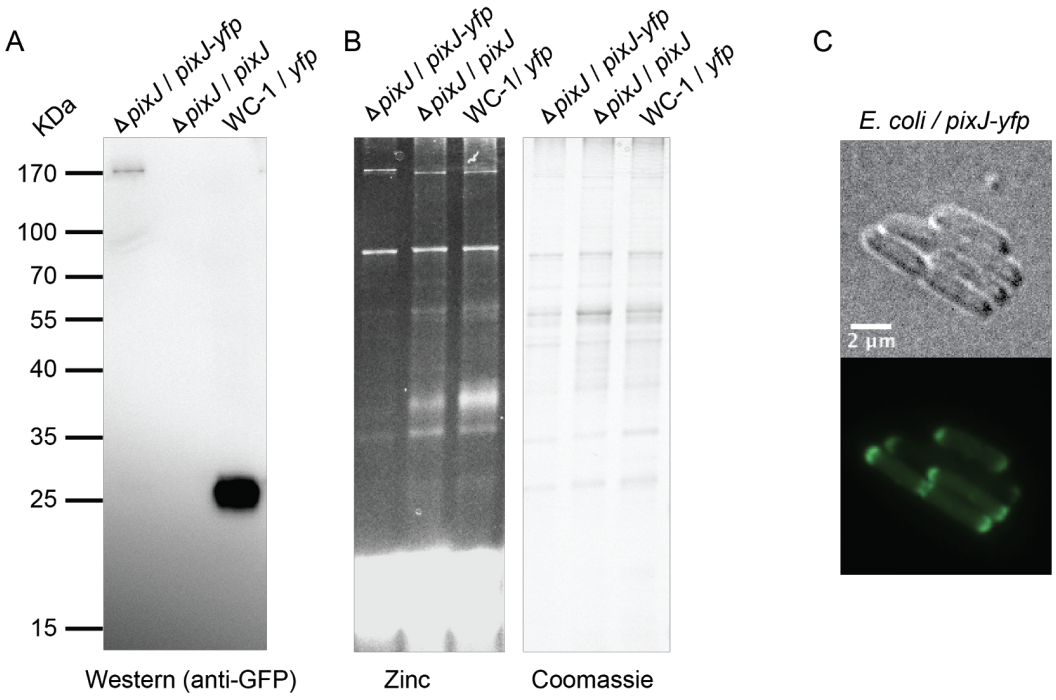

Fig. S14. Characterization of $PixJ_{Se}$-YFP. (A) Immunoblot performed with α-GFP as primary antibody. This result showed that a full-length $PixJ_{Se}$-YFP fusion (181 KDa) is expressed in UTEX 3055 and no protein degradation was detected. (B) Zinc blot shows $PixJ_{Se}$-YFP retains the ability to bind bilin. (C) Heterologously expressed $PixJ_{Se}$-YFP localized at cell poles of *E. coli* strain UU1581.

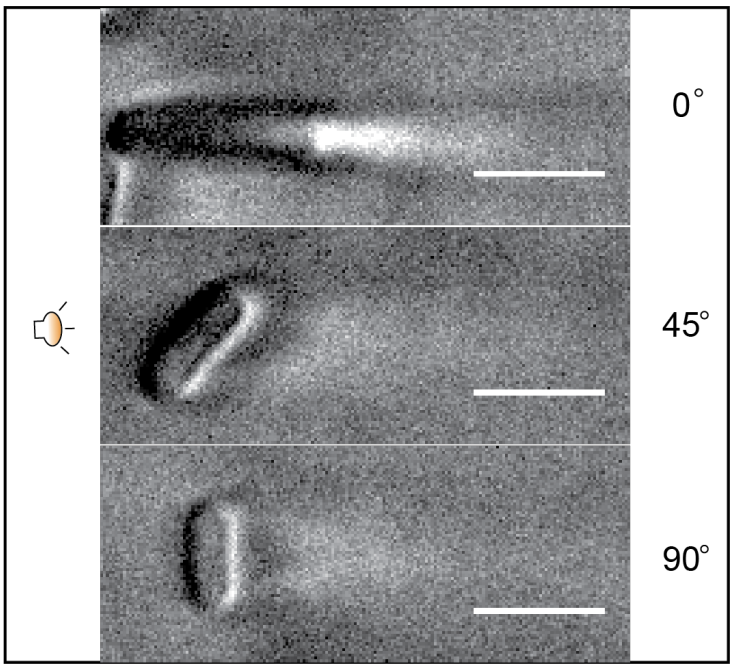

Fig. S15. Lensing effect of *S. elongatus* PCC 7942 cells at different orientations relative to the incident light direction. Cell sample was prepared as in Fig. S5 and imaged at 100x magnification. Scale bars = 3 μm.

Table S1. Genome information for *S. elongatus* PCC 7942 and UTEX 3055.

	PCC 7942			UTEX 3055		
	# base pairs	% GC	# ORFs	# base pairs	% GC	# ORFs
Chromosome	2,750,104	55	2621	2,767,524	55	2770
Large plasmid	46,366	53	50	89,249	51	97
PCC 7942 pANL	7,835	59	9			
UTEX 3055 plasmid				24,450	50	25

Table S2. Clock-related PCC 7942 genes identified in UTEX 3055.

PCC 7942	UTEX 3055 homolog	Annotation
synpcc7942_1218	UTEX 3055_1318	KaiA, circadian oscillator protein
synpcc7942_1217	UTEX 3055_1317	KaiB, circadian oscillator protein
synpcc7942_1216	UTEX 3055_1316	KaiC, circadian oscillator protein
synpcc7942_0095	UTEX 3055_0092	RpaA, two-component response regulator
synpcc7942_2114	UTEX 3055_2238	SasA, signal transduction histidine kinase
synpcc7942_0644	UTEX 3055_0779	CikA, GAF sensor signal transduction histidine kinase
synpcc7942_0480	UTEX 3055_0485	CikB, GAF sensor signal transduction histidine kinase
synpcc7942_0624	UTEX 3055_0759	LdpA, light-dependent period
synpcc7942_0677	UTEX 3055_0813	Pex, transcriptional regulator, PadR family
synpcc7942_0600	UTEX 3055_0735	PrkE, serine/threonine protein kinase
synpcc7942_1453	UTEX 3055_1555	RpaB, two-component response regulator, winged helix family
synpcc7942_1891	UTEX 3055_2009	LabA, uncharacterized conserved protein, 2C LabA/DUF88 family
synpcc7942_1168	UTEX 3055_1266	CpmA, circadian phase modifier
synpcc7942_2526	UTEX 3055_2679	ClpX, ATP-dependent Clp protease ATP-binding subunit
synpcc7942_2525	UTEX 3055_2678	ClpP, ATP-dependent Clp protease proteolytic subunit
synpcc7942_2160	UTEX 3055_2292	Nht1, alanine-glyoxylate aminotransferase apoenzyme
synpcc7942_2387	UTEX 3055_2539	IrcA, hypothetical protein / Cytochrome c
synpcc7942_1604	UTEX 3055_1596	CdpA, hypothetical protein
synpcc7942_1143	UTEX 3055_1241	LalA, hypothetical protein
Between synpcc7942_0095 and 0096	UTEX 3055_0093	Crm, circadian rhythm modulator

Table S3. Plasmids used in this study.

Plasmid	Description	Antibiotics	Source
8S23-L12	Tn*5*-insertion mutation of *pixI-2*	Km	(1)
8S23-E4	Tn*5*-insertion mutation of *pixG*	Km	(1)
8S23-H7	Tn*5*-insertion mutation of *pixH*	Km	(1)
8S42-B8	Tn*5*-insertion mutation of synpcc7942_1014	Km	(1)
8S26-H11	Tn*5*-insertion mutation of synpcc7942_1015	Km	(1)
8S26-O4	Tn*5*-insertion mutation of synpcc7942_1016	Km	(1)
pBAD-Cph1	P_{BAD} promoter, Cph1(N514)-producing plasmid	Ap	(11)
pKT271	P_{BAD} promoter, PCB-producing plasmid	Cm	(10)
pPL-PCB	$P_{lac/ara-1}$, PCB-producing plasmid	Km	(11)
pAM2105	P_{KaiB}-*luc* expressed from NS1	Cm	Lab collection
pAM2226	P_{KaiB}-*luc* expressed from NS2	SpSm	Lab collection
pAM4819	Cloning vector carrying *Aph*I cassette	Km	(3)
pAM4843	Cloning vector carrying an origin of replication for *E. coli.*	Ap	(3)
pAM4933	P_{conII}-yfp expressed from NS1	SpSm	(3)
pAM5431	P_{trc}-*SpSm-lacI-rrnB* expressed from NS1	SpSm	This work
pAM5472	PixG KO vector, derived from pAM4819 and pAM4843	Km	This work
pAM5473	PixH KO vector, derived from pAM4819 and pAM4843	Km	This work
pAM5474	Synpcc7942_2534 KO vector, derived from pAM4819 and pAM4843	Km	This work
pAM5475	P_{trc}-*pixL* (PCC 7942) expressed from NS1, derivative of pAM5431	SpSm	This work
pAM5476	P_{trc}-*pixJ* (PCC 7942) expressed from NS1, derivative of pAM5431	SpSm	This work
pAM5477	P_{trc}-*pixJ* expressed from NS1, derivative of pAM5431	SpSm	This work
pAM5478	P_{trc}-*pixL* expressed from NS1, derivative of pAM5431	SpSm	This work
pAM5479	P_{trc}-*pixG* expressed from NS1, derivative of pAM5431	SpSm	This work
pAM5480	P_{trc}-*pixH* expressed from NS1, derivative of pAM5431	SpSm	This work
pAM5481	PixJ KO vector, derived from pAM4819 and pAM4843	Km	This work
pAM5482	PixL KO vector, derived from pAM4819 and pAM4843	Km	This work
pAM 5483	PixI-1 KO vector, derived from pAM4819 and pAM4843	Km	This work
pAM5484	P_{trc}-$pixJ^{C300A}$ expressed from NS1, derivative of pAM5477	SpSm	This work
pAM5485	P_{trc}-$pixJ^{C644A}$ expressed from NS1, derivative of pAM5477	SpSm	This work
pAM5486	P_{trc}-$pixJ^{C816A}$ expressed from NS1, derivative of pAM5477	SpSm	This work
pAM5487	P_{trc}-$pixJ^{C988A}$ expressed from NS1, derivative of pAM5477	SpSm	This work
pAM5488	P_{trc}-$pixJ^{C472A, C644A}$ expressed from NS1, derivative of pAM5477	SpSm	This work
pAM5489	P_{trc}-$pixJ^{C300A, C816A}$ expressed from NS1, derivative of pAM5477	SpSm	This work
pAM5490	P_{trc}-$pixJ^{C816A, C988A}$ expressed from NS1, derivative of pAM5477	SpSm	This work
pAM5491	P_{trc}-$pixJ^{C300A, C472A, C644A}$ expressed from NS1, derivative of AM5477	SpSm	This work
pAM5492	P_{trc}-$pixJ^{C472A, C644A, C816A}$ expressed from NS1, derivative of AM5477	SpSm	This work
pAM5493	P_{trc}-$pixJ^{C300A, C472A, C644A, C816A}$ expressed from NS1, derivative of AM5477	SpSm	This work
pAM5494	P_{trc}-$pixJ^{C300A, C472A, C6444A, C988A}$ expressed from NS1, derivative of AM5477	SpSm	This work
pAM5495	P_{trc}-$pixJ^{C300A, C472A, C644A, C816A, C988A}$ expressed from NS1, derivative of AM5477	SpSm	This work
pAM5496	P_{trc}-$pixJ^{C644A, C816A}$ (GAF2,3 hybrid) expressed from NS1, derivative of AM5477	SpSm	This work
pAM5497	P_{trc}-*pixJ*-yfp expressed from NS1, derivative of AM5477	SpSm	This work
pAM5498	P_{BAD} promoter, $PixJ_{Se}$GAF2 producing plasmid	Ap	This work

Table S4. Cyanobacterial strains used in this study.

Strain	Genotype	Antibiotics	Source
AMC06	WT *S. elongatus* PCC 7942		Lab collection
AMC2388	WT *S. elongatus* UTEX 3055		This work
AMC2450	UTEX 3055_1014 (UGS 23G8)	Km	This work
AMC2492	*pixG*::Tn5 (UGS 22C11)	Km	This work
AMC2493	*pixH*::Tn5 (UGS 22C12)	Km	This work
AMC2494	Δ*pixI-1*::Km	Km	This work
AMC2495	*pixJ* (UGS 22D2)	Km	This work
AMC2496	Δ*pixJ*::Km	Km	This work
AMC2497	*pixL* with (UGS 22D3)	Km	This work
AMC2498	Δ*pixL*::Km	Km	This work
AMC2499	*pixI*-2 (UGS 22D4)	Km	This work
AMC2501	UTEX 3055_1015 (UGS 23G9)	Km	This work
AMC2502	AMC2496 (Δ*pixJ*::Km) and *pixJ* in NS1	Km SpSm	This work
AMC2503	AMC2496 with *pixJ*_C300A in NS1	Km SpSm	This work
AMC2504	AMC2496 with *pixJ*_C644A in NS1	Km SpSm	This work
AMC2505	AMC2496 with *pixJ*_C816A in NS1	Km SpSm	This work
AMC2506	AMC2496 with *pixJ*_C988A in NS1	Km SpSm	This work
AMC2507	AMC2496 with *pixJ*_C472A, C644A in NS1	Km SpSm	This work
AMC2508	AMC2496 with *pixJ*_C300A, C816A in NS1	Km SpSm	This work
AMC2509	AMC2496 with *pixJ*_C816A, C988A in NS1	Km SpSm	This work
AMC2510	AMC2496 with *pixJ*_C300A, C472A, C644A in NS1	Km SpSm	This work
AMC2511	AMC2496 with *pixJ*_C472A, C644A, C816A in NS1	Km SpSm	This work
AMC2512	AMC2496 with *pixJ*_C300A, C472A, C644A, C816A in NS1	Km SpSm	This work
AMC2513	AMC2496 with *pixJ*_C300A, C472A, C644A, C988A in NS1	Km SpSm	This work
AMC2514	AMC2496 with *pixJ*_C300A, C472A, C644A, C816A, C988A in NS1	Km SpSm	This work
AMC2515	AMC2496 with *pixJ*_C644A, C816A (GAF2, 3 hybrid) in NS1	Km SpSm	This work
AMC2516	AMC2496 with P_{trc}_*pixJ_yfp* in NS1	Km SpSm	This work
AMC2517	AMC2496 with *pixJ* from PCC 7942	Km SpSm	This work
AMC2518	AMC2496 with *pixL* from PCC 7942	Km SpSm	This work
AMC2519	AMC2497 with *pixL* in NS1	Km SpSm	This work
AM2520	P_{kaiB}::*luc* in NS1	SpSm	This work
AM2521	P_{kaiB}::*luc* in NS2	Cm	This work

Table S5. *E. coli* strains used in this study.

Strain	Genotype	Source
DH5α	F– Φ80*lacZ*ΔM15 Δ(*lacZYA-argF*) U169 *recA1 endA1 hsdR17* (rK–, mK+) *phoA supE44 λ– thi-1 gyrA96 relA1*	Lab collection
UU1581	(*flhD-flhA*)Δ*tr4*(*tsr*) Δ*7028 zdb::Tn5*(*trg*)Δ*100thr*(Am)-1 *leuB6 his*-4 *met*F(Am)*159 rpsL136 thi-1 ara-14 lacY1 mtl-1 xyl-1 xyl-5 tonA31 tsx-78*	Gift from J.S. Parkinson
LGM194	F- Δ*lacX74 galE thi rpsL* Δ*phoA* (Pvu II) Δ*ara714 leu::Tn10*	Lab collection
JM109	F′ *traD36 proA*$^{+}$*B*$^{+}$ *lacI*^{q} *Δ(lacZ)M15/ Δ(lac-proAB) glnV44 e14*$^{-}$ *gyrA96 recA1 relA1 endA1 thi hsdR17*	Lab collection

Movie S1. Formation of finger-like projections during UTEX 3055 phototaxis.

movie S2. Flow of UTEX 3055 cells moving toward light source.

Movie S3. Moving of finger tips toward light source.

Movie S4. UTEX 3055 cell movement under parallel gradient created from light source above cells.

Movie S5. UTEX 3055 cell movement under lateral illumination.

Movie S6. Movement of PCC 7942 cells under lateral illumination.

Movie S7. Lensing effect of UTEX 3055 cells during phototaxis.

Movie S8. Lensing effect of UTEX 3055Δ*pixJ* mutant during phototaxis.

References

1. Holtman CK, et al. (2005) High-throughput functional analysis of the *Synechococcus elongatus* PCC 7942 genome. *DNA Res* 12(2):103–115.

2. Chen Y, Holtman CK, Taton A, Golden SS (2012) Functional analysis of the *Synechococcus elongatus* PCC 7942 Genome. *Functional Genomics and Evolution of Photosynthetic Systems*, Advances in Photosynthesis and Respiration. (Springer, Dordrecht), pp 119–137.

3. Taton A, et al. (2014) Broad-host-range vector system for synthetic biology and biotechnology in cyanobacteria. *Nucleic Acids Res* 42(17):e136.

4. Sendersky E, Simkovsky R, Golden S, Schwarz R (2017) Quantification of Chlorophyll as a Proxy for Biofilm Formation in the Cyanobacterium *Synechococcus elongatus*. *BIO-PROTOCOL* 7(14). doi:10.21769/BioProtoc.2406.

5. Paintdakhi A, et al. (2016) Oufti: an integrated software package for high-accuracy, high-throughput quantitative microscopy analysis. *Mol Microbiol* 99(4):767–777.

6. Mackey SR, Ditty JL, Clerico EM, Golden SS (2007) Detection of rhythmic bioluminescence from luciferase reporters in cyanobacteria. *Methods Mol Biol* 362:115–129.

7. Yoshihara S, Katayama M, Geng X, Ikeuchi M (2004) Cyanobacterial phytochrome-like PixJ1 holoprotein shows novel reversible photoconversion between blue- and green-absorbing forms. *Plant Cell Physiol* 45(12):1729–1737.

8. Nagar E, et al. Type 4 pili are dispensable for biofilm development in the cyanobacterium *Synechococcus elongatus*. *Environmental Microbiology* 19(7):2862–2872.

9. Berkelman TR, Lagarias JC (1986) Visualization of bilin-linked peptides and proteins in polyacrylamide gels. *Anal Biochem* 156(1):194–201.

10. Angermayr SA, Gorchs Rovira A, Hellingwerf KJ (2015) Metabolic engineering of cyanobacteria for the synthesis of commodity products. *Trends Biotechnol* 33(6):352–361.

11. Gambetta GA, Lagarias JC (2001) Genetic engineering of phytochrome biosynthesis in bacteria. *Proc Natl Acad Sci USA* 98(19):10566–10571.